ARTICLE

# Organic–Inorganic Hybrids as Transparent Coatings for UV and X-ray Shielding

**Laura Mazzocchetti, Elisa Cortecchia, and Mariastella Scandola***

Dipartimento di Chimica "G. Ciamician", Università di Bologna and INSTM UdR Bologna, Via Selmi 2, 40126 Bologna, Italy

**ABSTRACT** This work reports the synthesis of new polymer–titania hybrids, where the organic phase is constituted by polyesters such as poly(ϵ-caprolactone), poly(D,L-lactic acid), and poly(L-lactic acid). In these hybrids, very strong interaction between the organic and inorganic domains is obtained through transesterification of ester moieties by titanium atoms, which leads to organotitanium esters. The influence of the structure of the polyester on the mode of its interaction with titania is also investigated. Hybrids with a range of solid-state properties, which depend on the starting polymer characteristics and on the inorganic-phase content, are obtained. Hybrids are applied as coatings on a variety of substrates. They show intrinsic optical transparency and the ability to completely block UV radiation in the range UVB and UV-A2. In particular, when applied to different textiles, the hybrids impart radiopacity to the fabrics, opening new perspectives in the field of personal protective clothing and equipment.

**KEYWORDS:** organic–inorganic hybrids • coating • radiopacity • UV filter • transparency • titania • polyester

## 1. INTRODUCTION

Performance improvement is one of the driving forces in materials science research (1, 2). Application of a functional coating layer is an easy way to modify the surface properties of materials. This procedure avoids undesired bulk property changes that might negatively affect a material's performance, while it allows the introduction of several functional properties associated with the coating formulation.

In this context, organic–inorganic hybrids (3–5) represent a smart class of new materials that can be easily applied as functional coatings. Hybrids can be regarded as a synergic combination of organic and inorganic compounds that benefit from ductility and low processing temperature, which is typical of polymers, as well as from high modulus, thermal stability, and low coefficients of thermal expansion distinctive of inorganic metal oxides. The interconnection between organic and inorganic domains, which is typical of the hybrid structure, confers to the material some additional features such as remarkable improvements in mechanical (6), thermal (7, 8), electrical (9), and magnetic properties (10). A classification of hybrid structures based on the type/strength of the organic–inorganic interaction has been proposed in a pioneering work by Sanchez and Ribot (4). When the inorganic domains are within nanometric dimensions, hybrids display optical transparency (11). Hybrid functional properties can be tuned by the convenient choice of the organic and inorganic components, and the final behavior can be adjusted by playing on their relative content. In this frame, the most suitable synthetic pathway to achieve a hybrid structure is represented by the sol–gel technique (12, 13), and the obtained materials are commonly named "ceramers" (CERAmics polyMERS) (14) or "ORMOCERs" (ORganically MOdified CERamics) (15).

Sol–gel is a process formerly developed for the production of metal oxides (16). It consists of hydrolysis and condensation reactions that, starting from metal alkoxide, lead to a metal oxide tridimensional network (13). The inclusion of appropriate polymers during the sol–gel process may lead to the formation of a strongly interconnected two-phase material, i.e., the hybrid. The sol–gel process needs to be carried out in a solvent, and it belongs to the so-called "wet chemistry" techniques: this feature allows hybrids to be easily applied as thin coating layers to a wide variety of substrates.

While a large number of polymers have been employed in ceramer synthesis (14, 17–28), the choice of the inorganic component is commonly addressed to silica (29) owing to the ease in handling silicon alkoxides during silica-based hybrid production. Although the high reactivity of transition-metal alkoxides implies some difficulties when they are used for hybrid preparation (13, 30, 31), the resulting material usually possesses some interesting additional features that are inherently associated with the obtained transition-metal oxide. For example, when titanium alkoxide is used for titania-containing hybrid preparation, it is shown that the resulting material displays some useful functional features such as X-ray- and UV-blocking properties (32). Hence, the use of such hybrids in the form of coatings may represent a smart solution to the problem of radiographic traceability of endoprosthetic devices that are presently coated either by rather complex deposition technologies (33, 34) or in high-temperature conditions (35) that are unsuitable for polymeric equipment. In addition, the application of such hybrid coatings on textiles should lead to the production of

* To whom correspondence should be addressed. E-mail: mariastella.scandola@unibo.it. Tel: +39 051 2099577. Fax: +39 051 2099456.
Received for review December 11, 2008 and accepted February 11, 2009

DOI: 10.1021/am800230j



Published on Web 03/04/2009

personal protective clothing for medical staff exposed to X-ray radiation such as during angiographic surgery (36, 37). Obviously, in order to cope with different application requirements, hybrid features have to be carefully tuned for each specific use.

This work reports the synthesis and characterization of new hybrids made of titania and polyesters with different solid-state behavior, i.e., poly(caprolactone) and poly(lactic acid) [both PLLA and PDLLA]. The results of the characterization study shed new light on the interactions that set in during hybrid synthesis between organic and inorganic phases, confirming the hypothesis previously formulated in connection with hybrids containing titania and poly[1,4-butylene glutarate] (38).

This paper also discusses the properties of hybrids coated on substrates of different nature and shape and their potential use as easily applicable protective coatings.

## 2. EXPERIMENTAL SECTION

**2.1. Materials.** Chloroform (Aldrich), poly($\epsilon$-caprolactone) (PCL; Tone 787, Union Carbide, $\bar{M}_w$ = 75 000 Da, PDI = 4.9), poly(L-lactic acid) (PLLA; Lacea H-100-E, $\bar{M}_w$ = 84 000 Da, PDI = 1.7), poly(D,L-lactic acid) (PDLLA, Resomer R 203 H Boheringer, $\bar{M}_w$ = 36 000 Da, PDI = 2.6), poly(1,4-butylene glutarate) (PBG; Aldrich, $\bar{M}_w$ = 3700 Da, PDI = 2.8), and titanium tetraisopropoxide (TIPT; Aldrich) were used without further purification.

**2.2. Hybrid Synthesis and Coating on Flat Substrates.** The precursors of the organic and inorganic phases, i.e., the polymer and TIPT, respectively, are dissolved in different weight ratios (polymer + TITP total weight = 1 g) in 3 mL of the solvent ($CHCl_3$). The hybrids are labeled H-P*X*, where P stands for the polymer acronym (PBG, PCL, PDLLA, and PLLA) and label *X* represents the weight percentage of the polymer (*X* = 10, 25, 50, or 75) in the sol−gel feed.

The synthesis of hybrid H-PCL50 is described as an example: 1.0 g of TIPT is added to 2 mL of $CHCl_3$ (solution 1). In a separate container 1.0 g of PCL is dissolved in 4 mL of $CHCl_3$ (solution 2). After complete polymer dissolution, solution 2 is added to solution 1 under vigorous stirring. The obtained clear mixture (solution 3) then either is poured into a Teflon Petri dish to produce a bulk hybrid sample or, alternatively, is coated on different flat substrates such as aluminum, steel, copper, glass, cellulose acetate, polypropylene (PP), or tetrafluoroethylene (Teflon) sheets. Coating is obtained either by dipping the substrate in the solution or by casting the solution on the substrate and removing the excess solution with the aid of a sliding glass rod (Doctor Blade Method). After 2 h at room temperature (RT), a transparent solid layer (maximum thickness 10 $\mu$m) forms on all different substrates. Then the coated samples are thermally treated for 1 h in an oven at 110 °C. The bulk hybrids prepared in the Petri dishes, as described above, are aged for 24 h at RT (solidification) prior to a 2 h oven treatment at 110 °C (curing).

**2.3. Hybrid Coating on Textiles.** In order to achieve application of a hybrid coating on textiles, a synthetic procedure analogous to that described above is followed, with the only difference being a greater amount of solvent (10 vs 3 mL of $CHCl_3$) used to dissolve 1 g of hybrid precursors (polymer + TITP).

As an example, the procedure to synthesize the H-PBG50 coating is described: 0.5 g of TIPT is added to 1 mL of $CHCl_3$ (solution 1), while in a separate container 0.5 g of PBG is dissolved in 9 mL of $CHCl_3$ (solution 2). After complete polymer dissolution, solution 2 is added to solution 1 under vigorous stirring and the obtained mixture is allowed to stir for 1 min (solution 3). Then, small samples (2 cm × 2 cm) of different fabrics (cotton, silk, wool, and polyester) are immersed in solution 3, from which they are retrieved after 15 s. A portion of solution 3 is also cast on a Teflon sheet in order to obtain the hybrid in the form of a thin layer, which can be used as a reference material for the coatings. Both the thin films cast on Teflon and the coated textiles are aged for 2 h at RT and further thermally treated for 1 h in an oven at 110 °C.

**2.4. Characterization Techniques.** IR spectra are recorded on a Nicolet 380 FT-IR, with 32 scans and 4 $cm^{-1}$ resolution. Solid insoluble samples are ground with KBr (1 mg of sample/100 mg of KBr) and pelletized under pressure, while analysis of the starting polymers (PBG, PCL, PDLLA, and PLLA) is performed by casting a few drops of a polymer solution in chloroform on a KBr disk and allowing solvent evaporation prior to measurement. All such samples are dried overnight in a desiccator over $P_2O_5$ before Fourier transform IR (FT-IR) analysis.

Differential scanning calorimetry (DSC) measurements are carried out with a TA DSC-Q100 apparatus, equipped with a liquid-nitrogen cooling system accessory. Samples (about 5 mg) are subjected to three subsequent heating runs at 20 °C/min from −100 °C up to +100 °C. Controlled cooling at 10 °C/min is applied after the first heating scan, while quench cooling is performed after the second heating scan. $T_g$ values are taken at half-height of the glass transition heat capacity step.

The pencil hardness of hybrids coated onto rectangular aluminum plates is evaluated according to the standard test method ASTM D 3363 (39).

Thermogravimetric (TGA) measurements are carried out using a TGA 2950 (TA Instruments). The analyses are performed by heating at 10 °C/min from RT to 600 °C under an air flow.

UV−vis spectra are recorded on a Cary 1E (Varian) spectrophotometer in the range 200−700 nm with a scan rate of 600 nm/min. Transparent PP film (31 $\mu$m thick) is used as the substrate on which a hybrid layer (4−6 $\mu$m thick) is coated. Transmittance of the coated PP is measured with changing wavelength, and $\lambda_{50}$ is the wavelength at which the transmittance is reduced to less than 50%.

Scanning electron microscopy (SEM) observations are carried out using a Philips 515 scanning electron microscope at 15.0 kV. The coated and uncoated fabrics are laid down on aluminum stubs using conductive adhesive tape and are sputter-coated with gold prior to measurements.

The textile sample area is evaluated through analysis of its digital picture by means of Zeiss AxioVision 3.0 software. The hybrid load (HL) on textiles is quantified using an analytical electronic Sartorius RC210D balance (reproducibility ± 0.02 mg).

Radiographic images are recorded on a mammographic apparatus (Diamond MGX, Instrumentarium Co. Imaging Division) equipped with a Varian M113SP radiogenic tube. The experimental parameters are 22 keV, 4 mA/s, and 21 cm sample-to-detector distance.

## 3. RESULTS AND DISCUSSION

**3.1. Hybrid Bulk Synthesis and Characterization.** In an earlier work by the authors (38), an organic−inorganic hybrid was prepared via the sol−gel process starting from a dihydroxy-terminated polyester (PBG) and a titanium alkoxide (TIPT) as titania precursors. In the cited work, it was demonstrated that a strong interaction between the polymer and the in situ forming titania was achieved via the transesterification reaction of the polymer chain, leading to organotitanium esters connecting organic and inorganic domains. Because the transesterification reaction does not require the presence of any specific chain end group, in

**Scheme 1**

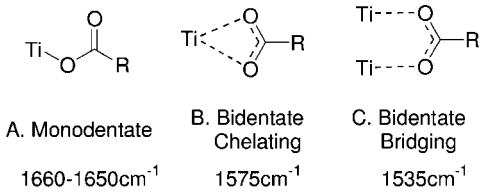


principle any polyester able to dissolve in a good solvent for the titania precursor should be able to lead to hybrid structures such as those earlier observed with dihydroxy-terminated PBG.

The correctness of the above hypothesis is investigated in the present work. The same procedure formerly adopted by the authors for low-molecular-weight ($\bar{M}_w$ ca. 3600 Da), dihydroxy-terminated PBG (38) is now applied in the synthesis of hybrids using high-molecular-weight polyesters with different solid-state properties as organic-phase precursors. PCL is chosen because of its low glass transition temperature ($T_g \approx -60$ °C) and low melting crystal phase ($T_m$ around 55−65 °C) (40), while PLA, used both as a PLLA homopolymer and as a PDLLA copolymer, has $T_g = 55$ °C and is glassy at RT. Moreover, PLLA is able to crystallize ($T_m = 185-215$ °C), whereas PDLLA is totally amorphous (40).

The hybrids are produced via the sol−gel process in chloroform, a good solvent for the polymers and for the titania precursor employed (TIPT). It is well established that titanium alkoxides are highly reactive toward nucleophiles and that they can give rise to uncontrolled fast reactions (13). As an example, the presence of water in the reaction environment often leads to instantaneous titania precipitation. Takahashi and co-workers thoroughly studied the reactivity of transition-metal alkoxides (31), and they demonstrated the possibility of running sol−gel reactions without water addition. In fact, they observed that water, which is indeed required for hydrolysis to occur, can be obtained in a convenient amount and concentration from air humidity, thus avoiding any undesired titania precipitation.

In this work, the hybrids are synthesized using a 50:50 (w/w) polymer/TIPT feed ratio. The bulk materials recovered from Teflon Petri dishes after thermal curing, as described in the Experimental Section, are analyzed by FT-IR spectroscopy in order to investigate organic−inorganic phase interactions. Earlier work on PBG-containing hybrids (38) showed that titanium-driven transesterification leads to the formation of a new carbonyl stretching absorption band in the FT-IR spectrum, centered at lower wavenumbers than the traditional ester carbonyl stretching (1535 vs 1740 $cm^{-1}$). It is well-known that a carbonyl group complexing an electron-deficient atom shifts its IR absorption to lower wavenumbers to an extent that depends on the mode of interaction (41−43), as depicted in Scheme 1. The mentioned new band observed in PBG-based hybrids was attributed (38) to the stretching of the C═O moiety interacting with the titanium atom in agreement with previous assignments (31). Figure 1 compares the FT-IR spectra of the presently synthesized hybrids, focused on the carbonyl stretching absorption range, with those of the respective

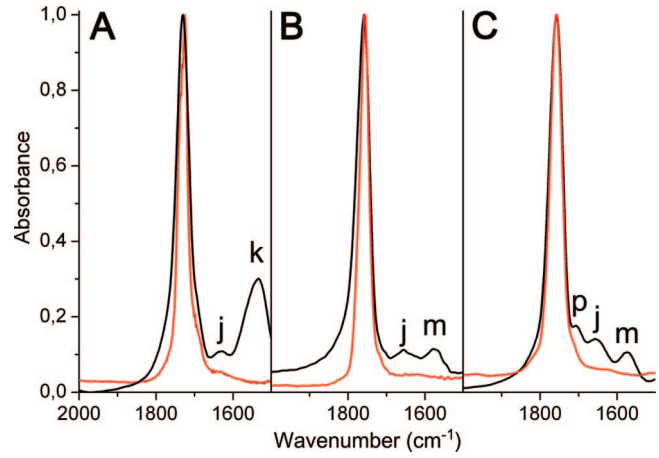


**FIGURE 1. FT-IR spectra, focused on the 1500−2000 $cm^{-1}$ carbonyl region of (A) PCL (red) and H-PCL50 (black), (B) PLLA (red) and H-PLLA50 (black), and (C) PDLLA (red) and H-PDLLA50 (black). Letters identify peaks at different wavelengths: j, 1650−1660 $cm^{-1}$; k, 1535 $cm^{-1}$; m, 1575 $cm^{-1}$; p, 1700 $cm^{-1}$.**

plain polymers. Besides the expected carbonyl absorption at 1740 $cm^{-1}$, all hybrids in Figure 1 display a new band in the range of 1660−1650 $cm^{-1}$ (absorption j) that, according to the literature (43), can be attributed to monodentate titanium ester carbonyl (Scheme 1A). The presence of such a band, not detected in the previously synthesized H-PBG hybrids, may be due to the high molecular weight of the present polymers, which may hinder further carbonyl coordination expansion after transesterification. Moreover, all hybrids show a second signal at even lower wavenumbers (absorption k at 1535 $cm^{-1}$ and absorption m at 1575 $cm^{-1}$).

The new band (k) at 1535 $cm^{-1}$ in the FT-IR spectrum of H-PCL50 (Figure 1A) lies at the same wavenumber as the absorption found in the spectrum of the previously analyzed H-PBG50 (38). Accordingly, absorption k in H-PCL50 is attributed to the organotitanium ester carboxylate, which additionally interacts with titanium atoms through the carbonyl oxygen, giving rise to a bidentate bridging structure (31), as sketched in Scheme 1C. The presence of the 1535 $cm^{-1}$ band in the spectrum of the hybrid containing the high-molecular-weight polyester is further confirmation that the chemical bond forms via chain scission at the ester linkage.

The spectra of H-PLLA50 and H-PDLLA50 (parts B and C of Figure 1, respectively) show the additional absorption m at 1575 $cm^{-1}$, i.e., at slightly higher wavenumbers than absorption k of hybrid H-PCL50 (Figure 1A). According to the literature, absorption m in the two PLA-based hybrids might be ascribed to a bidentate chelating structure, as depicted in Scheme 1B. Worth noting is that in the case of H-PDLLA50 a third new band at 1700 $cm^{-1}$ is observed (absorption p), which can be attributed to some free carboxylic acid moiety that forms during the transesterification process.

The different FT-IR behavior of hybrids H-PLLA and H-PDLLA with respect to hybrids H-PBG and H-PCL may be due to the presence, in the former hybrids, of the methyl group in the α position to the carboxyl moiety. The sterical hindrance of the α substituent inhibits to some extent the transesterification reaction on the carbonyl, as evidenced by

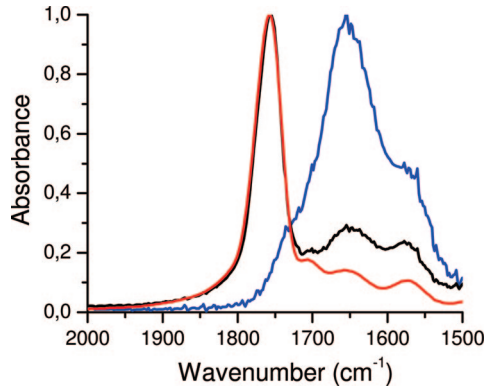


**FIGURE 2. FT-IR spectra focused on the 1500−2000 $cm^{-1}$ carbonyl regions of H-PDLLA50 (red), H-PDLLA25 (black), and H-PDLLA10 (blue). Spectra are normalized with respect to the intensity of the main carbonyl stretching signal, i.e., 1740 $cm^{-1}$ for H-PDLLA50 and H-PDLLA25 and 1650 $cm^{-1}$ for H-PDLLA10.**

the lower intensity of bands j + m in PLA hybrids with respect to bands j + k in H-PCL50. Moreover, when titanium coordination expansion occurs, the mode of interaction is affected by the presence of a bulk group close to the carboxyl moiety and the bidentate chelating structure (band m) is preferred to a bidentate bridging one (band k).

With the aim of confirming that the observed new bands in PLA hybrids originate from the interaction between organic and inorganic components, two new hybrids with higher inorganic content are investigated, namely, H-PDLLA25 and H-PDLLA10, whose FT-IR spectra are reported in Figure 2. For the sake of comparison, the spectrum of H-PDLLA50 (same as that in Figure 1C) is also displayed in Figure 2. Spectra are normalized with respect to the intensity of the main carbonyl signal, that is, 1740 $cm^{-1}$ for H-PDLLA50 and H-PDLLA25 and 1650 $cm^{-1}$ for H-PDLLA10. With increasing titania content, a clear increase of the intensity of the new bands in the range of 1500−1720 $cm^{-1}$ is observed, showing that the new signals are titania-related. It is clear that the new bands grow at the expense of the organic ester absorption (1740 $cm^{-1}$), which is totally absent in H-PDLLA10, thus confirming the involvement of polyester carboxylate groups in the interaction with titanium atoms.

The chain mobility and phase behavior of the polymeric component of the hybrids is investigated by DSC. Table 1 compares the results of DSC measurements on H-PCL50, H-PLLA50, and H-PDLLA50 with those of the respective plain polymers (PCL, PLLA, and PDLLA). For the sake of comparison, Table 1 also reports DSC data of the previously synthesized hybrid H-PBG50 (for synthesis and characterization, see ref 38).

Analysis of the DSC data in Table 1 shows that neither of the polyesters containing a linear monomer (PCL and PBG) leads to hybrids containing a crystal phase, although both plain polymers are easily crystallizable in identical experimental conditions. Conversely, PLLA develops crystallinity in hybrid H-PLLA50. The different behavior observed can be attributed to the different ability of the "linear" polyesters and of PLLA to interact with titanium atoms, which has been discussed above in connection with the FT-IR results. Owing to its pending methyl group close to carbonyl, PLLA interacts with titanium to a lower degree, thus maintaining its crystallizing ability in the hybrid, whereas crystallization of PCL and PBG is prevented by the strong interaction between these polymers and the inorganic phase. A similar behavior has been previously reported not only for PBG-containing hybrids (38) but also for silica-based hybrids containing a crystallizable polymer (44−47), where crystallization of the polymeric component was found to be strongly reduced or even totally inhibited owing to organic−inorganic phase interaction.

As concerns the glass transition of the hybrids, all previously studied silica ceramers synthesized from end-functionalized precursors (44−47) showed an increase of $T_g$ of the polymer component upon hybrid synthesis, which reflects a decrease of the mobility of the polymer chains whose ends are locked into the silica network. The $T_g$ data in Table 1 show for H-PCL50, H-PDLLA50, and H-PLLA50 an opposite trend, with $T_g$ being lower in the hybrids than in the respective precursor polymers. In the present hybrids, a degree of chain anchoring by the titania phase can be reasonably expected because of the aforementioned polymer−inorganic phase interactions. However, the molecular weight of the polymeric phase decreases as a consequence of the transesterification reactions occurring during hybrid synthesis, and this leads to an opposite effect on $T_g$. The interplay of the two phenomena determines the final hybrid $T_g$ value. Table 1 also shows that the transition width ($\Delta T_g$) is larger in the hybrids than in the respective polymers, implying that the polymer−titania interactions lead to broadening of the relaxation time distribution, as expected.

The mechanical behavior of the synthesized hybrids at RT is likely to reflect the aforementioned thermal properties. In particular, an important property of coatings, i.e., for the type of application that is foreseen for the present hybrids, is hardness. Hence, the pencil hardness of the hybrids, evaluated by a standard ASTM test (D3363) (39) that determines the hardest pencil that does not fracture or gouge the coating, is reported in Table 1. The results show that the hardness increases in the order H-PCL50 < H-PBG50 < H-PDLLA50 < H-PLLA50. This behavior can be rationalized by taking into account the $T_g$ values in Table 1, showing that PCL and PBG are rubbery at RT, while the two PLAs are glassy. Moreover, H-PLLA50 also contains a crystal phase that enhances the hardness of this hybrid with respect to that of H-PDLLA50. The present results suggest that it is possible to tune hybrid mechanical properties through selection of a polymeric phase with suitable thermal properties.

**3.2. Hybrid Coating on Flat Surfaces.** The versatility of the synthesized hybrids in yielding materials with different hardness and stiffness and the particularly mild and easy conditions required to carry out the sol−gel process (16) make this class of products excellent candidates to be applied as coating layers on a wide variety of substrates. Hence, in this work hybrids made of PBG (38), PCL, PLLA, or PDLLA and titania are applied as coating layers on a wide variety of flat substrates.

**Table 1. Thermal Properties of Hybrids and of the Corresponding Polyester Precursors**

| | TGA[a] | | | DSC[b] | | | |
|---|---|---|---|---|---|---|---|
| sample | residue (%) | $T_g$ (°C) | $\Delta T_g$[c] (°C) | $\Delta C_p$ (J/g °C) | $T_m$ (°C) | $\Delta H_m$ (J/g) | pencil hardness[d] |
| PCL | <0.5 | −63 | 7 | 0.13 | 56 | 71 | |
| H-PCL50 | 21.2 | −65 | 10 | 0.39 | | | <6B |
| PLLA | <0.5 | 70 | 5 | 0.22 | 163 | 36 | |
| H-PLLA50 | 23.6 | 64 | 21 | 0.18 | 158 | 24 | 3H |
| PDLLA | <0.5 | 51 | 5 | 0.57 | | | |
| H-PDLLA50 | | 46 | 13 | 0.27 | | | HB |
| PBG | <0.5 | −72 | 8 | 0.68 | 13 | 44 | |
| H-PBG50 | 22.5 | −61 | 12 | 0.40 | | | 6B |

[a] Experimental solid residue at 600 °C evaluated from TGA experiments run in air. [b] From the second heating scan after quench cooling. [c] Glass transition width. [d] Measured according to ASTM D 3363, on hybrids coated on aluminum plates.

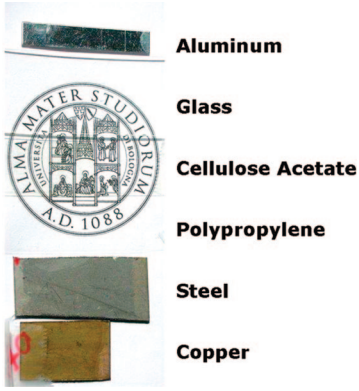


**FIGURE 3. Hybrid H-DLLA50 cast on different substrates. Application on transparent substrates outlines a coating transparency to visible light.**

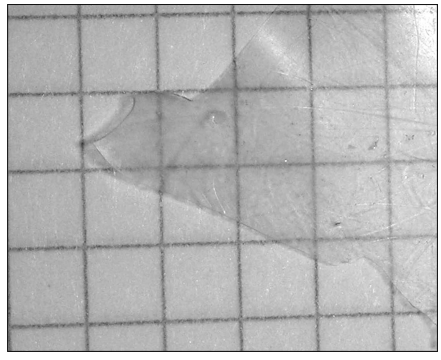

**FIGURE 4. Hybrid H-PBG15 in bulk is transparent to visible light despite the high titania content ($TiO_2$ = 61.4%).**

As displayed in Figure 3 for H-PDLLA50 as an example, hybrids with different formulations (polymer type, polymer/TIPT feed ratio, and precursor/solvent ratio) are easily applied (by casting or dipping) to a range of different materials such as aluminum, steel, copper, glass, cellulose acetate, and PP. It is clearly observed that when the hybrid is cast on a transparent substrate, the resulting coated material maintains transparency to visible light. This is mainly due to the nanometric dimension of titania domains that are not able to scatter radiation with wavelengths in the range of visible light (11). Transparency is maintained up to high titania loads, as demonstrated in Figure 4 by the hybrid H-PBG15, which has been produced starting from a feed ratio polymer/TITP = 15/85 and contains more than 60% by weight of titania.

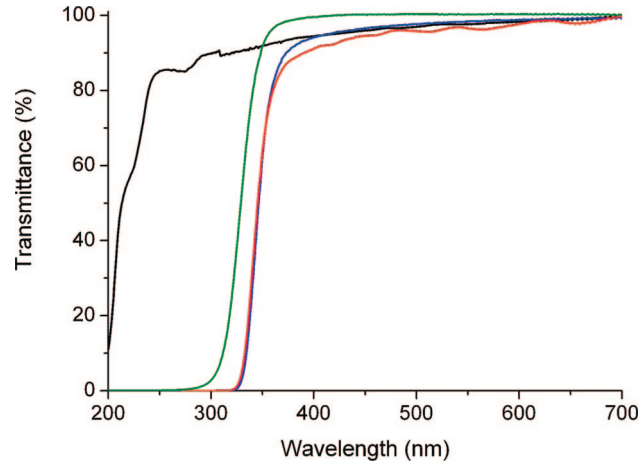


**FIGURE 5. Comparison of the UV−vis spectrum of a PP sheet (31 $\mu$m thick, black) with those of a PP sheet coated with H-PBG75 (6-$\mu$m-thick coating, red), H-PBG50 (5-$\mu$m-thick coating, blue), and H-PBG25 (4-$\mu$m-thick coating, green).**

Hybrids show very good adhesion toward all surfaces on which they have been coated in this study (plastics, metals, and glass) except Teflon, a substrate from which they can be easily peeled off. The latter support is thus used to produce very thin self-standing hybrid layers, whose thickness (around 10 $\mu$m) is comparable to that of the coating layers applied to plastics, metals, and glass. These self-standing thin hybrids, which are the reference materials for the coatings, are characterized by FT-IR, DSC, and TGA, and no substantial differences between such samples and the previously discussed bulk materials are observed.

UV−vis absorption properties of hybrids in the form of thin layers coated on a transparent PP sheet (31 $\mu$m thick) are tested. As an example, Figure 5 shows UV−vis transmittance spectra of three PBG hybrids with different titania contents, namely, H-PBG75, H-PBG50, and H-PBG25, coated on PP. For the sake of comparison, the spectrum of plain PP is also reported, showing transmittance higher than 90% along the entire UVB/ UVA range (280 nm < $\lambda$ < 400 nm). In the same frequency range, hybrids H-PBG75, H-PBG50, and H-PBG25 are able to cut off a large fraction of the UV radiation. In particular, H-PBG50 and H-PBG25 layers (5 and 4 $\mu$m thick, respectively) cast on PP are completely opaque to UV radiation up to $\lambda$ = 325 nm, i.e., over the whole so-called UVB range (280−315 nm) (48). Although UVB rays

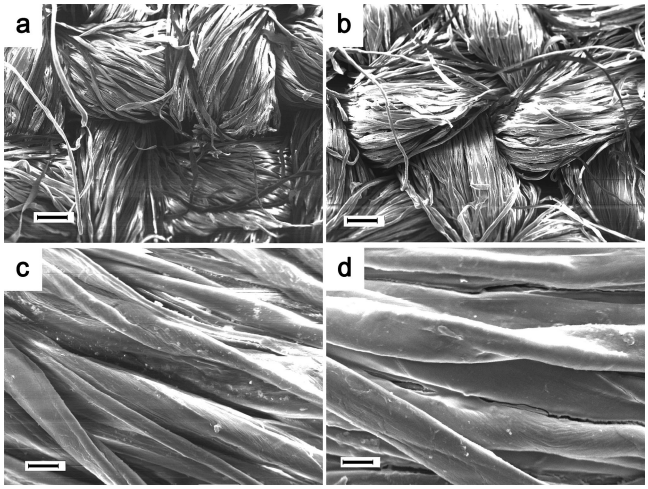


**FIGURE 6. SEM micrographs at different magnification of cotton fabric (a and c) and of cotton fabric coated with H-PBG50 (b and d). Bar: 100 $\mu$m in parts a and b and 10 $\mu$m in parts c and d.**

represent a small fraction of the extraterrestrial solar radiation, because of their high energy, they are responsible for most of the harmful effects of exposure to sunlight (49). The synthesized hybrids are also able to cut off a large part of the UVA spectrum, i.e., the UV-A2 range (48). In particular, for wavelengths lower than 345 nm, the transmitted radiation intensity is reduced down to 50% ($\lambda_{50} = 345$ nm). It is worth noting that although the titania content in H-PBG75 is rather small (75 wt % of PBG and 25% of TIPT in the feed correspond to about 9% of titania in the final hybrid) a mere 6-$\mu$m-thick layer of this hybrid is able to halve the intensity of UV radiation with $\lambda \leq 330$ nm.

**3.3. Hybrid Coatings on Textiles.** Because hybrids are produced by the sol–gel process, the entire spectrum of wet-coating techniques (spin coating, dip coating, spray coating, etc.) is available for the deposition of these materials as coating layers. It is thus possible to foresee a wide range of applications for such hybrids on a number of substrates, no matter their actual shape.

In this work, hybrid deposition via dip coating on complex substrates such as textiles made of different fibers, namely, cotton, silk, wool, and polyester, has been attempted. PBG is chosen as the organic-phase constituent of the hybrid, because of its low $T_g$ and low melting crystal phase ($T_m <$ RT). PBG-based hybrids are expected to be able to comply with yarn flexibility, and indeed all fabrics that have been coated with such hybrids show a quite pleasant hand. SEM micrographs of cotton coated with H-PBG50 are shown in Figure 6, where they are compared with pictures of the untreated fabric at the same magnification. Remarkably, no appreciable differences between coated and uncoated fabrics are observed. It is interesting to note that the hybrid (pictures b and d) is able to coat single fibers of the yarn rather than coating the yarn as a whole. Openings between yarns are maintained, and fabric breathability is preserved.

Interesting results are obtained from TGA measurements on hybrid-coated fabrics (cotton, wool, silk, and polyester). The plain uncoated fabrics are also analyzed, showing in all cases of very small, if any, solid residue at the end of the TGA measurement (600 °C) under air purge. On the contrary, upon heating up to 600 °C in air, all coated fabrics yield a solid residue, whose value reflects the composition and amount of hybrid coated on the fabric. Hereafter, as an example, the behavior of coated cotton fabrics, whose TGA results are listed in Table 2, is discussed in depth.

The weight of the coated fabric can be considered as arising from two independent components, namely, the cotton yarn and the hybrid loaded onto the cellulosic support. Upon heating of the plain cotton yarn up to 600 °C in air purge, a constant solid residue $SR_{cot} = 1.7\%$ by weight is obtained. The plain hybrids in bulk form are also analyzed under the same conditions, and the solid residue found at 600 °C ($SR_{bulk}^{meas}$) is reported in Table 2. Table 2 also lists the solid residue ($SR_{bulk}^{exp}$) expected on the assumption that during the sol–gel process complete hydrolysis of the inorganic-phase precursor has occurred and, upon oxidation and volatilization of all of the organic material, only $TiO_2$ is left over at 600 °C.

$SR_{bulk}^{exp}$ is calculated as follows: (38):

$$SR_{bulk}^{exp} = \frac{X_{TIPT}\dfrac{MW_{TiO_2}}{MW_{TIPT}}}{X_{PBG} + X_{TIPT}\dfrac{MW_{TiO_2}}{MW_{TIPT}}} \qquad (1)$$

where $X_{PBG}$ and $X_{TIPT}$ are the weight fractions of the organic and inorganic precursors in the feed and $MW_{TiO_2}$and $MW_{TIPT}$ are the molecular weights of titania and of TIPT, respectively. In line with earlier results (38, 45), the values of $SR_{bulk}^{meas}$ and $SR_{bulk}^{exp}$ are in good agreement, confirming that the hybrid composition can be directly adjusted by playing with the feed composition.

The amount of hybrid coated on the cotton fabrics, gravimetrically estimated, is reported as the percentage of hybrid load (HL) in Table 2. The values of HL vary between ca. 13% to about 23%, and it is interesting to note that, notwithstanding such differences, the solid residue at 600 °C of the coated fabrics measured by TGA (Table 2) increases with an increase in the TIPT content, i.e., in the order H-PBG75 > H-PBG50 > H-PBG25. Such experimentally determined residues may be compared with the value expected for a hybrid-coated cotton ($SR_{HybCot}^{exp}$), calculated according to the following equation:

$$SR_{HybCot}^{exp} = SR_{bulk}^{meas}\frac{HL}{100} + SR_{cot}\frac{100 - HL}{100} \qquad (2)$$

where $SR_{bulk}^{meas}$ refers to a bulk hybrid obtained from the same sol–gel feed as the one applied on cotton fabrics. Equation 2 takes into account the contribution to the solid residue from thermal degradation of both hybrid and cotton fibers, assuming that hybrid formation on textile substrates proceeds in the same manner as that in the bulk. The results reported in Table 2 show substantial agreement between the

**Table 2. Solid Residue from TGA of Bulk H-PBG Hybrids and of Hybrid-Coated Cotton**

| | | | | TGA | |
|---|---|---|---|---|---|
| abbrev | PBG in feed (%) | sample type | HL[a] (%) | measured residue[b] (%) | expected residue (%) |
| H-PBG25 | 25 | bulk | | 44.5 | 45.8[c] |
| | 25 | coated fabric | 13.3 | 9.9 | 7.5[d] |
| H-PBG50 | 50 | bulk | | 22.5 | 21.9[c] |
| | 50 | coated fabric | 22.7 | 6.9 | 6.4[d] |
| H-PBG75 | 75 | bulk | | 11.2 | 8.6[c] |
| | 75 | coated fabric | 17.5 | 3.2 | 3.4[d] |

[a] Percentage of hybrid load, defined as the hybrid weight fraction in the final sample, gravimetrically determined by weighing the dried fabric sample before and after hybrid coating. [b] Experimental solid residue at 600 °C evaluated from TGA experiments run in air. [c] $SR^{Th}_{bulk}$ calculated according to eq 1. [d] $SR^{Th}_{HybCot}$ calculated according to eq 2.

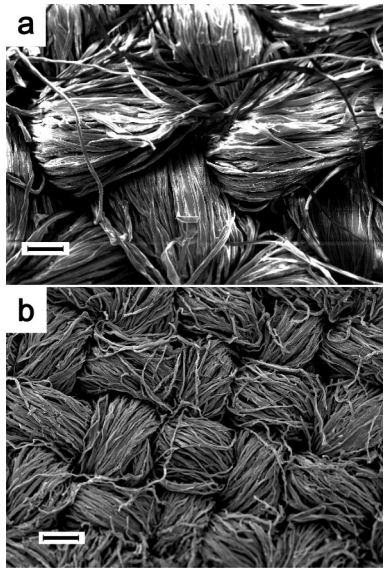


**FIGURE 7. SEM micrographs at the same magnification of cotton fabric coated with H-PBG50 before (a) and after TGA measurement up to 600 °C in air (b). Bar: 100 $\mu$m.**

calculated residue ($SR^{exp}_{HybCot}$) and experimental results, demonstrating that the composition of the hybrid, in situ synthesized from precursors adsorbed onto the fabric, is that expected based on their mutual weight ratio. No significant composition change due to precursor preferential loading by capillary sorption is observed, thus showing that the final coating composition can be easily defined by playing on the sol–gel feed composition.

Earlier results (38, 45) have demonstrated that in both titania- and silica-based hybrids the solid residue obtained after TGA experiments in air up to 600 °C is the plain metal oxide. In this work, as mentioned above, almost no significant solid residue ($SR_{cot} = 1.7$ wt %) is found in plain cotton; hence, it can be safely assumed that the TGA residue of coated fabrics at 600 °C (Table 2) is mainly composed of titania. Figure 7 shows SEM micrographs (at the same magnification) of cotton coated with H-PBG50, taken before and after a TGA run up to 600 °C in air. It is evident that the solid residue after TGA experiments keeps the exact texture as the starting sample, although notably reduced in size. A SEM micrograph at higher magnification of the TGA solid residue (Figure 8) showing the yarn cross section clearly illustrates that the fibrous-looking residue in the front view of Figure 7b is indeed an empty titania envelope that

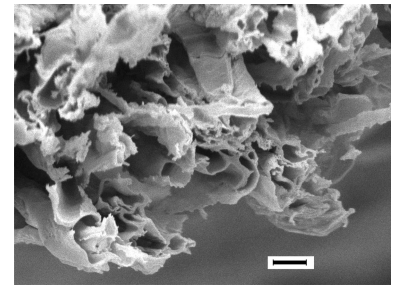

**FIGURE 8. SEM micrograph of cotton fabric coated with H-PBG50 after TGA experiment up to 600 °C in air (side view). Bar: 5 $\mu$m.**

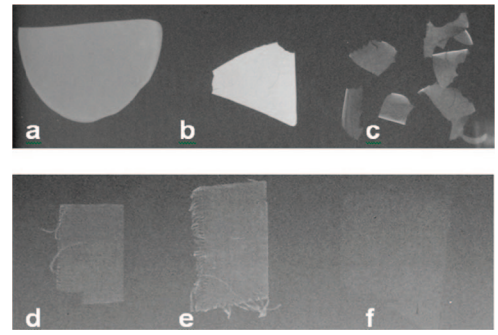


**FIGURE 9. Radiographic images of (a) bulk H-PBG50 (640 $\mu$m thick), (b) bulk H-PBG25 (490 $\mu$m thick), (c) bulk H-PBG25 (35 $\mu$m thick), (d) cotton fabric coated with H-PBG50, (e) cotton fabric coated with H-PBG25, and (f) uncoated cotton fabric.**

maintains the fiber shape after thermal decomposition and volatilization of both the polymeric component of the hybrid coating and the inner cellulosic fibers.

In a previous work (38), the authors showed that bulk H-PBG hybrids are opaque to X-ray radiation. This property, like the above-discussed UV-blocking activity, is peculiar to the inorganic phase. Thus, it can be speculated that radiopacity will characterize any titania-containing hybrid, to an extent that depends on the actual amount of titania per hybrid unit volume. On the assumption that radiopacity can be transferred to fabrics by the simple described procedure of hybrid coating, radiographic images of coated fabrics are taken with mammographic equipment. Figure 9 shows radiographs of bulk H-PBG hybrids and of hybrid-coated cotton. For the sake of comparison, the radiograph of plain cotton is also reported.

It is interesting to note that good contrast against the background can be obtained with a thick (640 $\mu$m) H-PBG50 bulk sample (Figure 9a); an acceptable contrast can also be

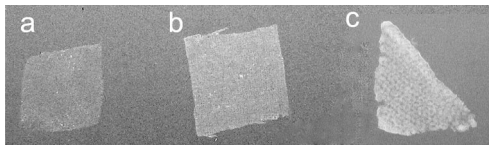


**FIGURE 10. Radiographic images of (a) polyester coated with H-PBG25, (b) silk coated with H-PBG25, and (c) wool coated with H-PBG50.**

obtained with a thinner (35 $\mu$m) sample of the H-PBG25 hybrid (Figure 9c) because, as expected, the material enrichment in the inorganic component allows thinning of the hybrid layer while still maintaining radiopacity. Obviously, a much thicker H-PBG25 sample (490 $\mu$m) provides a much stronger contrast (Figure 9b). In contrast to the plain uncoated cotton, which is practically undetectable under radiographic conditions (Figure 9f), application of the hybrid coating on cotton fabric gives, as expected, X-ray visibility to the textile. In parts d and e of Figure 9, cottons coated with hybrids characterized by a different compositions, namely, H-PBG50 and H-PBG25, respectively, are reported. It is worth noting that similar radiographic contrasts of the two samples may be ascribed (see Table 2) to an almost double load onto the fabric of the hybrid with lower titania content (H-PBG50).

In addition to cotton, other fabrics become radiopaque upon coating with the hybrids, as shown in Figure 10 in the case of polyester and silk coated with H-PBG25 and of wool coated with H-PBG50. In order to compare the radiopacity of different hybrid-coated textile substrates, besides the hybrid composition, also the specific loading capacity of each substrate must be taken into account. Hence, the HL per fabric unit area ($L_A$, mg/cm$^2$) is defined as follows:

$$L_A = \frac{\Delta m}{a} \tag{3}$$

where $\Delta m$ is the HL on the fabric, gravimetrically determined as the fabric weight increment upon hybrid coating (with weights before and after coating being taken after careful drying), and $a$ is the area of the fabric sample measured from a digital picture via software (see the Experimental Section).

The effect of the $L_A$ parameter is evident when comparing in Figure 10 the pictures of polyester and silk fabrics coated with the same hybrid (H-PBG25). The lower contrast of the coated polyester sample originates from its lower normalized HL ($L_A$ = 3.44 mg/cm$^2$) compared with that of the brighter coated silk textile ($L_A$ = 6.17 mg/cm$^2$). It is worth mentioning that the normalized loading of cotton fabric coated with the same H-PBG25 hybrid, whose radiograph is displayed in Figure 9e, is $L_A$ = 3.76 mg/cm$^2$. A picture comparison shows that cotton (Figure 9e) and polyester (Figure 10a), i.e., two fabrics with similar load per unit area, display similar radiopacity. On the other hand, the reason for the strong radiographic contrast of the wool fabric in Figure 10, despite the fact that it is coated with H-PBG50 (a hybrid with a smaller titania content than H-PBG-25), lies on the great loading capacity of wool ($L_A$ = 28.84 mg/cm$^2$).

The above examples show the concomitant effect on the final fabric radiopacity both of the fiber ability to upload the hybrid precursors during the synthetic procedure and of the fraction of titania in the hybrid formulation.

The results discussed above demonstrate an easy route to providing radiopacity to textiles with many possible applications, for example, in the field of personal protective equipment. It is likely that workers involved in everyday radiation exposition may take advantage of garments able to block X-rays, much like everyone exposed to prolonged sunlight may benefit from protection against UV radiation.

## 4. CONCLUSIONS

The synthesis of new titania-containing hybrids, where the organic phase is constituted by different polyesters such as PCL, PDLLA, and PLLA, has provided further evidence that transesterification of ester moieties by titanium atoms leads to the formation of the organotitanium ester, resulting in very strong interaction between the hybrid organic and inorganic domains. Hybrids obtained from such diverse polyesters display different properties, which depend on the starting polymer characteristics and on the inorganic-phase content. They can thus be applied as coatings in different fields, according to the degree of stiffness required by the specific application.

Hybrids coated on transparent substrates show their intrinsic optical transparency and their ability to completely block UV radiation in the range of UVB and UV-A2. Moreover, when textiles are coated with hybrids, they become radiopaque, thus paving the way to the production of new personal protective clothing and equipment.

**Acknowledgment.** The authors gratefully thank Prof. Stefano Mignani and Rita Luciani (Centro Mammografico, Policlinico Universitario Sant'Orsola, Bologna University) for the radiographs.

### REFERENCES AND NOTES

(1) Backov, R. *Soft Matter* **2006**, *2*, 452–464.
(2) Prouzet, E.; Ravaine, S.; Sanchez, C.; Backov, R. *New J. Chem.* **2008**, *32*, 1284–1299.
(3) Judeinstein, P.; Sanchez, C. *J. Mater. Chem.* **1996**, *6*, 511–525.
(4) Sanchez, C.; Ribot, F. *New J. Chem.* **1994**, *18*, 1007–1047.
(5) Yano, S.; Iwata, K.; Kurita, K. *Mater. Sci. Eng., C* **1998**, *6*, 75–90.
(6) Okada, A.; Usuki, A. *Mater. Sci. Eng., C* **1995**, *3*, 109–115.
(7) Gilman, J. W.; Jackson, C. L.; Morgan, A. B.; Harris, R.; Manias, E.; Giannelis, E. P.; Wuthenow, M.; Hilton, D.; Phillips, S. H. *Chem. Mater.* **2000**, *12*, 1866–1873.
(8) Porter, D.; Metcalfe, E.; Thomas, M. J. K. *Fire Mater.* **2000**, *24*, 45–52.
(9) Armes, S. P. *Polym. News* **1995**, *20*, 233–237.
(10) Godovski, D. Y. *Adv. Polym. Sci.* **1995**, *119*, 78–122.
(11) Caseri, W. *Macromol. Rapid Commun.* **2000**, *21*, 705–722.
(12) Brinker, J. C., Sherer, G. In *Sol–Gel Science: The Physics and Chemistry of Sol–Gel Processing*; Academic Press: San Diego, 1990.
(13) Livage, J.; Henry, M.; Sanchez, C. *Prog. Solid State Chem.* **1988**, *18*, 259–341.
(14) Wilkes, G. L.; Orler, B.; Huang, H. *Polym. Prepr. (Am. Chem. Soc., Div. Polym. Chem.)* **1985**, *26*, 300–301.
(15) Schmidt, H. *J. Non-Cryst. Solids* **1985**, *73*, 681–691.
(16) Hench, L. L.; West, J. K. *Chem. Rev.* **1990**, *90*, 33–72.
(17) Huang, H.; Orler, B.; Wilkes, G. L. *Macromolecules* **1987**, *20*, 1322–1330.

(18) Surivet, F.; Thanh, M. L.; Pascault, J. P.; Mai, C. *Macromolecules* **1992**, *25*, 5742–5751.
(19) Kohjiya, S.; Ochiai, K.; Yamashita, S. *J. Non-Cryst. Solids* **1990**, *119*, 132–135.
(20) Huang, H.; Wilkes, G. L. *Polym. Bull.* **1987**, *18*, 455–462.
(21) Brennan, A. B.; Wang, B.; Rodrigues, D. E.; Wilkes, G. L. *J. Inorg. Organomet. Polym.* **1991**, *1*, 167–187.
(22) Brennan, A. B.; Wilkes, G. L. *Polymer* **1991**, *32*, 733–739.
(23) Tian, D.; Dubois, P.; Jerome, R. *J. Polym. Sci., Part A: Polym. Chem.* **1997**, *35*, 2295–2305.
(24) Tian, D.; Dubois, P.; Jerome, R. *Polymer* **1996**, *37*, 3983–3987.
(25) Tian, D.; Blacher, S.; Dubois, P.; Jerome, R. *Polymer* **1998**, *39*, 855–864.
(26) Saegusa, T. *J. Macromol. Sci. A* **1991**, *28*, 817–829.
(27) Noell, J. L. W.; Wilkes, G. L.; Mohanty, D. K.; McGrath, J. E. *J. Appl. Polym. Sci.* **1990**, *40*, 1177–1194.
(28) Messori, M.; Toselli, M.; Pilati, F.; Fabbri, E.; Fabbri, P.; Pasquali, L.; Nannarone, S. *Polymer* **2004**, *45*, 805–813.
(29) Kickelbick, G. *Prog. Polym. Sci.* **2003**, *28*, 83–114.
(30) Kallala, M.; Sanchez, C.; Cabane, B. *Phys. Rev. E* **1993**, *48*, 3692–3704.
(31) Takahashi, R.; Takenaka, S.; Sato, S.; Sodesawa, T.; Ogura, K.; Nakanishi, K. *J. Chem. Soc., Faraday Trans.* **1998**, *94*, 3161–3168.
(32) Scandola, M.; Mazzocchetti, L. PCT Patent Application WO2008/132691A2, 2008.
(33) Dobson, P. J. U.S. Patent 5,876,783, 1999.
(34) Sahagian, R. U.S. Patent 7,077,837, 2006.
(35) Bearinger, C. R.; Camilletti, R. C.; Haluska, L. A.; Michael, K. W. U.S. Patent 5,399,441, 1995.
(36) Bashore, T. M. *Am. Heart. J.* **2004**, *147*, 375–378.
(37) Thierens, H.; Reynaert, N.; Bacher, K.; van Eijkeren, M.; Taeymans, Y. *Int. J. Radiat. Oncol., Biol., Phys.* **2004**, *60*, 678–685.
(38) Mazzocchetti, L.; Scandola, M.; Pollicino, A. *Polymer* **2008**, *49*, 5215–5224.
(39) ASTM D 3363, 2005.
(40) In *Polymer Handbook*, 4th ed.; Brandrup, J., Immergut, E. H.,Grulke, E. A., Eds.; John Wiley and Sons, Inc.: New York, 1999.
(41) Boettcher, S. W.; Bartl, M. H.; Hu, J. G.; Stucky, G. D. *J. Am. Chem. Soc.* **2005**, *127*, 9721–9730.
(42) Boettcher, S. W.; Fan, J.; Tsung, C. K.; Shi, Q.; Stucky, G. D. *Acc. Chem. Res.* **2007**, *40*, 784–792.
(43) Hagan, D. B.; Leng, F. J.; Smith, P. M.; Snow, M.; Watson, A. *Int. J. Cosmet. Sci* **1997**, *19*, 271–280.
(44) Mazzocchetti, L.; Scandola, M.; Amerio, E.; Malucelli, G.; Marano, C. *Macromol. Chem. Phys.* **2006**, *207*, 2103–2111.
(45) Mazzocchetti, L.; Sandri, S.; Scandola, M.; Bergia, A.; Zuccheri, G. *Biomacromolecules* **2007**, *8*, 672–678.
(46) Ceccorulli, G.; Zini, E.; Scandola, M. *Macromol. Chem. Phys.* **2006**, *207*, 864–869.
(47) Malucelli, G.; Priola, A.; Sangermano, M.; Amerio, E.; Zini, E.; Fabbri, E. *Polymer* **2005**, *46*, 2872–2879.
(48) CIE Report 134/1, **1999**.
(49) Canada, J.; Esteve, A.; Marin, M. J.; Utrillas, M. P.; Tena, F.; Maitinez-Lozano, J. A. *Int. J. Climat.* **2008**, *28*, 693–702.

AM800230J